UNIVERSITY OF
BATH

Link to publication

University of Bath

Cloud Motion Analysis Using Multichannel Correlation-Relaxation Labeling

Adrian N. Evans

Abstract—**Cloud motion vectors derived from sequences of remotely sensed data are widely used by numerical weather prediction models and other meteorological and climatic applications. One approach to computing cloud motion vectors is the correlation-relaxation labeling technique, in which a set of candidate vectors for each template is refined using relaxation labeling to provide a local smoothness constraint. In this letter, an extension of the correlation-relaxation labeling framework to tracking clouds in multichannel imagery is presented. As this multichannel approach takes advantage of the diversity between channels, it has the potential for producing motion vectors with a superior quality and coverage than can be achieved by any individual channel. Results for visible and infrared images from Meteostat Second Generation confirm the benefits of the multichannel approach.**

Index Terms—**Cloud tracking, Meteostat Second Generation, motion analysis, multichannel images.**

I. INTRODUCTION

THE ANALYSIS of cloud motion in remotely sensed imagery is a challenging problem due to the nonrigid nature of the motion. Traditional approaches include template matching, in which templates from the first image are matched against all positions in the second image that are within a defined search area. The motion vector is then determined by the best match position. When the match measure employed is the cross-correlation coefficient (CCC), the result is the well-known maximum cross-correlation (MCC) method that has been a widely used operational method for deriving cloud-motion winds [1]. Other approaches to solving the correspondence problem in remotely sensed cloud sequences include the use of artificial neural networks to match contour shape descriptors [2] and image warping. More recently, Mukherjee and Acton have demonstrated a scale-space classification scheme for cloud tracking [3]. In this approach, pixels are clustered by applying a fuzzy c-means algorithm to scale-space vectors produced by area morphological operators. Correspondences for points on the boundary of the cloud mass with the minimum temperature are then established by minimizing a disparity-based cost function.

Despite these recent developments, the operational use of template-matching methods persists, although direct application of the MCC technique suffers from several disadvantages.

In particular, the underlying assumption that the correlation surface is unimodal does not hold for many remotely sensed images, which are characterized by low contrast and nonrigid motion. This drawback was overcome by correlation-relaxation labeling, in which relaxation labeling is applied to a set of candidate vectors for each template to produce a locally smooth motion field [4]. In [5], the CCC was shown to produce better candidate vectors that require fewer iterations of the relaxation procedure to improve the motion estimates than other computationally cheaper matching functions. The benefits of incorporating robust ordinal measures, based on the relative rank of intensities, within the correlation-relaxation framework for cloud tracking have also been investigated [6].

Zhou *et al.* present an analysis of the three-dimensional (3-D) nonrigid motion and structure of cloud sequences using the visible channel of the Geostationary Operational Environmental Satellite (GOES) Imager [7]. They propose an iterative approach that employs error of fit functions containing both local and global information. Here, the local information is captured by affine models, and the global analysis is based on the assumption of smooth motion and the dynamics of fluid flows. Although this approach is impressive, producing dense motion estimates from a single-channel sequence, the results given in [7] are derived from an input sequence with a sampling rate of 1 frame/min (GOES-9 operating in Super Rapid Scan Mode), and its performance with sequences with lower temporal resolutions remains to be established. This means, for example, that it cannot readily be applied to the analysis of sequences such as those produced by Meteostat Second Generation (MSG) that have a sampling rate of 1 frame/15 min.

Whereas the work of Zhou *et al.* [7] was applied to the visible GOES channel, Velden *et al.* use multichannel GOES sequences to derive 3-D cloud motion vectors [8]. In this approach, selected targets within the infrared and water vapor channels are assigned initial heights using their equivalent blackbody temperatures. Displacements, and hence velocity vectors, are generated by finding the minimum sum of squares between the target and the search positions. The vectors then undergo the postprocessing steps of height reassessment and quality control.

The application area for the technique presented in [8] is the tracking of Atlantic tropical cyclones. When a more global analysis of wind vectors is required, such as an input for numerical weather prediction (NWP) models, the resolving ability of this approach, and that of [7], may be computationally prohibitive. The technique presented in this letter is relatively efficient and makes use of multichannel data. However, rather than assign heights to the vectors from different channels,

the approach adopted is to exploit the diversity between the visible and infrared channels, which essentially image the same physical cloud structure, to produce dense two-dimensional motion vector fields with a reasonable computational cost. As such, it is suitable for large-scale analysis of cloud motion patterns. In particular, the correlation-relaxation labeling technique for motion estimation, which has been shown to be appropriate for analyzing nonrigid motion in remotely sensed images, is extended to accommodate candidate motion vectors from multiple channels. This new multichannel cloud motion estimation technique is described in Section II, and its application to the analysis of MSG images of the North Atlantic is investigated in Section III. Finally, conclusions are drawn in Section IV.

II. MULTICHANNEL CORRELATION-RELAXATION LABELING

The multichannel correlation-relaxation labeling framework used in this work is based on that described in [9]. The technique has three main stages: 1) template matching is used to determine a number of candidate matches for templates from each channel; 2) relaxation labeling is used to select the most appropriate of the candidate matches by applying a local smoothness constraint; and 3) a postfilter is used to replace vectors that are still inconsistent with the local flow. These stages are discussed in more detail below.

The image to be analyzed is first split into nonoverlapping blocks of equal size, termed templates. In single-channel correlation-relaxation labeling algorithms, up to n candidate motion vectors are found for each template, typically by selecting the n match positions with the highest CCC. The actual number of candidate vectors for a given template may be less than n as the CCC must exceed a predetermined threshold value to qualify as a potential match.

To combine candidate vectors from multiple channels, various approaches have been investigated, including taking the top n/c matches from each channel, where c is the number of channels, and selecting candidate matches that perform well in all channels. However, the scheme adopted here is to allow the candidate vectors from different channels to compete at the initial candidate selection stage by simply selecting the top n matches regardless of which channel they come from. In practice, this is achieved by finding the maximum of the CCCs from all channels at each match position and then selecting the n highest, provided they meet the qualifying criterion.

Normalizing the set of correlation coefficients for each template gives rise to the initial match probabilities required for the relaxation labeling stage. This is achieved by

$$P^{(0)}(J \to j) = \frac{\rho(J \to j)}{\sum_{\lambda \in \mathcal{C}_J} \rho(J \to \lambda)} \quad (1)$$

where $P^{(0)}(J \to j)$ is the initial probability of template J being assigned candidate vector j, $\mathcal{C}_J$ is the set of candidate vectors for template J, and $\rho(J \to j)$ is the CCC for the proposed match $J \to j$.

Probability updating is achieved by the iterative nonlinear relaxation formula

$$P^{(n+1)}(J \to j) = \frac{P^{(n)}(J \to j)Q(J \to j)}{\sum_{\lambda \in \mathcal{C}_J} P^{(n)}(J \to \lambda)Q(J \to \lambda)} \quad (2)$$

in which $Q(J \to j)$ is the support function that assesses the compatibility of the proposed labeling $J \to j$ with those within the local neighborhood of template J. Here, the local neighborhood is simply defined as those templates that are four- or eight-connected neighbors of J, denoted by $\mathcal{N}_J$. $Q(J \to j)$ is then given by

$$Q(J \to j) = \prod_{I \in \mathcal{N}_J} \sum_{i \in \mathcal{C}_I} P^{(n)}(I \to i)R(J \to j, I \to i) \quad (3)$$

where the mutual information $R(J \to j, I \to i)$ measures the similarity between the two velocity vectors associated with the labelings $J \to j$ and $I \to i$. To calculate R, a simplified form of the expression from [9] is used, i.e.,

$$R(J \to j, I \to i) = \exp\left(-\frac{|x_{J \to j} - x_{I \to i}|}{\sigma}\right)$$
$$\cdot \exp\left(-\frac{|y_{J \to j} - y_{I \to i}|}{\sigma}\right) \quad (4)$$

where $x_{J \to j}$ and $y_{J \to j}$ are the x and y components of the candidate vector $J \to j$, and σ is a constant that controls the rate of convergence. Unlike [4] and [9], this simplified formulation for R does not include a term that relates to the distance between feature points or templates. This is because the only templates to be considered in (3) are connected neighbors of template J. Therefore, the distance term can be considered to be constant.

The relaxation procedure is applied for a fixed number of iterations, or until a convergence criterion is met, and the candidate vector with the highest probability is assigned to each template, producing a motion field in which the vectors are locally consistent. However, as the relaxation algorithm does not include a null class, exceptions can occur for templates that do not have any candidate vectors that are consistent with the local flow. In these cases, the best result the relaxation algorithm can achieve is to select the least inconsistent vector. To remove these inconsistencies, a conditional vector median filter is applied. The filter first assesses the compatibility of the vector for each template with the vector median of its connected neighbors using (4), where the vector median is the vector with the minimum sum of distances to all other vectors in the set [10]. If the compatibility is below a predetermined threshold, the original vector is replaced by the vector median. The vector median post filter is an improvement upon that of [9] as it considers both channels jointly and is uniquely defined for an even number of samples.

III. EXPERIMENTAL RESULTS

The effectiveness of the new cloud motion analysis technique was investigated by application to two high-resolution channels of the MSG radiometer. Fig. 1 shows the visible channel of a high-resolution MSG image covering Europe and the North
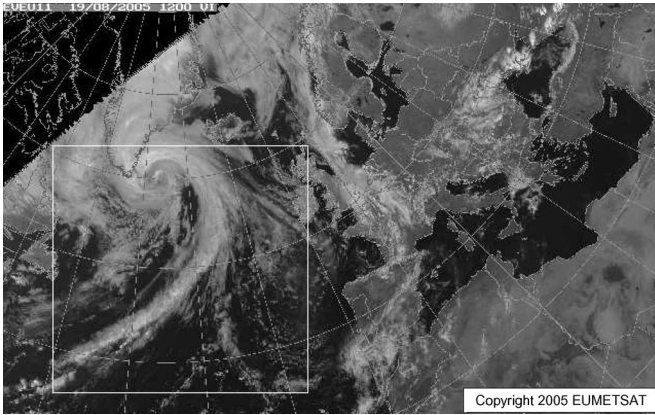
Fig. 1.   Visible channel of MSG high-resolution image, taken at 12:00 UT on August 19, 2005. Region of interest marked in white.

Fig. 3.   PSU/NCAR MM5 model result for 12:00 UT on August 19, 2005. The background color is proportional to the integrated cloud water, and the wind vectors are for the pressure level with the greatest cloud water content.

(a)   (b)

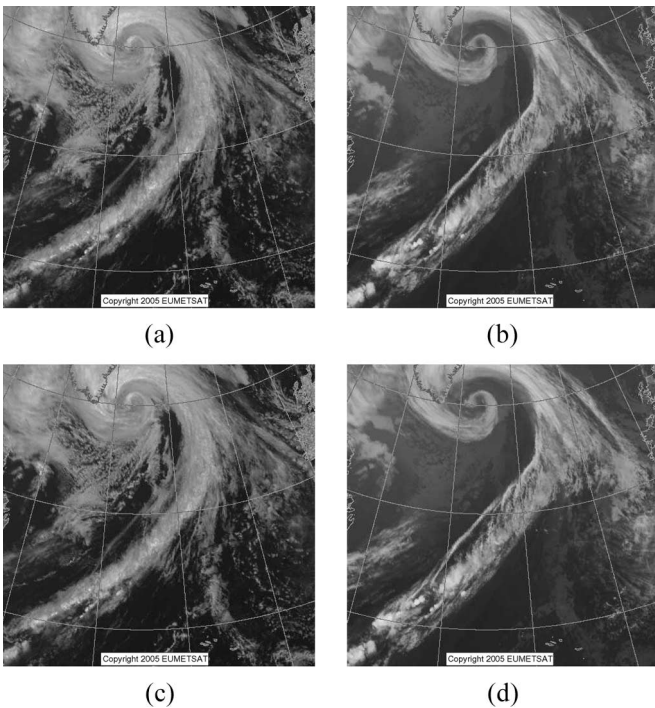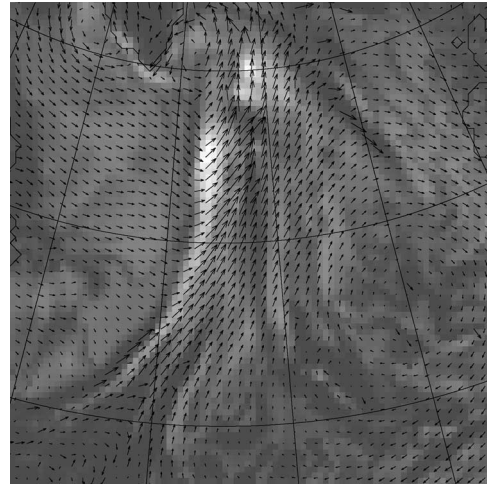(c)   (d)

Fig. 2.   Visible and infrared MSG channels for region of interest from Fig. 1. (a) Visible at 12:00 UT. (b) Infrared at 12:00 UT. (c) Visible at 12:15 UT. (d) Infrared at 12:15 UT.

used for visual comparison with the results of the multichannel correlation-relaxation algorithms.

For all experiments, the region of interest from each channel of the 12:00 Universal Time (UT) image shown in Fig. 2 was split into 62×60 nonoverlapping templates of size 8×8 pixels. Each template was then matched over a ± 8 search area in the corresponding channel of the 12:15 UT image. As the resolution of the MSG images is in the order of 3 km^2/pixel for the range of latitudes considered, this search range allows the tracking of clouds with velocities of up 100 km/h. The motion vectors corresponding to the MCC positions for the visible, infrared, and maximum of both channels are shown in Fig. 4(a), (c), and (e), respectively. Although the visible and infrared channels show general agreement with the model vectors, with some structure evident in both, there are regions where the vectors for one channel are clearly more consistent than for the other. Selecting the best vector regardless of the channel in which it occurred [Fig. 4(e)] produces a smoother flow, although there are still many local inconsistencies. In this image, 1620 vectors were from the visible channel and 2100 from the infrared channel, with a distribution as shown in Fig. 5(a).

Fig. 4(b), (d), and (f) shows the motion fields after applying 16 iterations of the relaxation algorithm to sets of up to 15 candidate vectors for each template. The threshold to qualify as a candidate vector was $\rho = 0.2$, and the parameter $\sigma = 250$ in (4). The single-channel relaxation results [Fig. 4(b) and (d)] are clearly an improvement on those of the MCC method and demonstrate the benefits conferred by the relaxation process. As the quality of the relaxed motion field depends on the quality of the candidate vectors, the single-channel results cannot find a locally consistent field in the absence of suitable candidates. Here, the difference between channels is mainly manifested as locally inconsistent vectors. Using sets of candidate vectors derived from both channels as the input to the relaxation algorithm produces the result in Fig. 4(f), with the channel that each relaxed vector is associated with shown in Fig. 5(b). Comparing Fig. 4 with the model wind vectors of Fig. 3 shows that the smoother, more locally consistent motion fields show better

Atlantic, with a 480×496 region of interest marked. The visible and infrared channels for the region of interest at time separation of 15 min shown in Fig. 2 form the inputs for the experimental investigation. Evaluating the performance of cloud motion estimation techniques is problematic as the exact motion between frames is not known. Visual examination of the image pairs shown in Fig. 2 can be used to manually validate the motion vectors but is time consuming. Alternatively, the output of an NWP model can be used to provide an approximation of the ground-truth motion field. Fig. 3 shows the output from the PSU/NCAR MM5 model for the same time and date as Fig. 1. The system was run on a polar stereographic grid with a grid scale of 35 km and a 12-h spin-up period. Although the projection of Fig. 3 differs from that of the MSG images, it provides a good indication of the true wind flow and can be
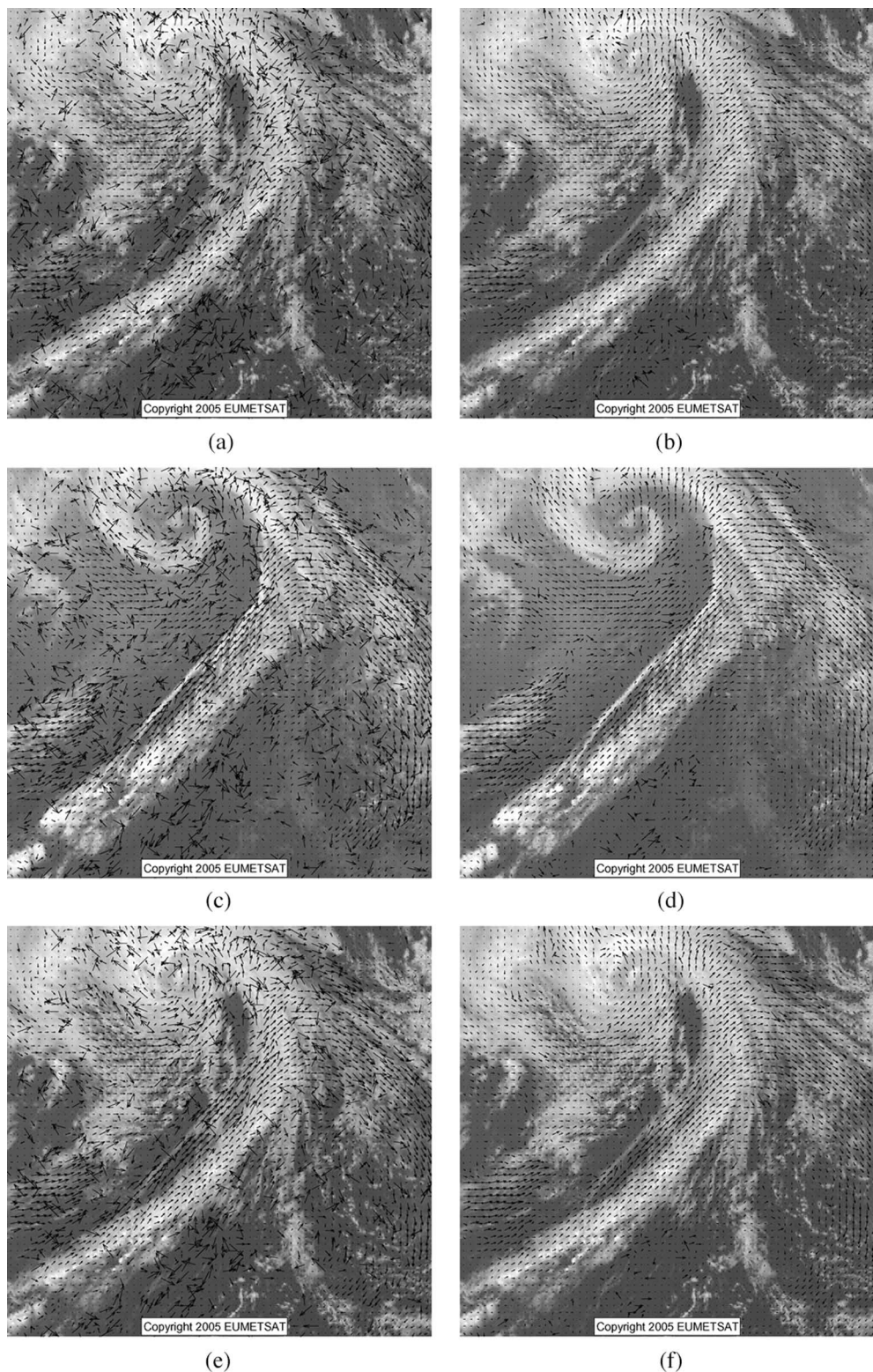
Fig. 4. MCC and correlation-relaxation results. Vectors at twice actual size for display purposes. (a) MCC for visible channel. (b) Relaxation result for visible channel. (c) MCC for infrared channel. (d) Relaxation result for infrared channel. (e) MCC for both channels. (f) Relaxation result for both channels.

agreement. The smoothness of a motion field can be quantified by its vector entropy, which can be estimated by the number of bits needed for lossless encoding. Table I presents the vector entropy of the motion fields from Fig. 4, calculated using the encoding scheme of the H.263 video-encoding standard [11], and confirms the advantage of the multichannel approach over

the use of individual channels. However, Fig. 4(f) still contains a small number of local outliers where neither channel can provide appropriate vectors for the candidate set. Applying the post filter to Fig. 4(f) with a threshold of 0.97 produces the final result in Fig. 6, which has a dense, locally consistent motion field that shows good agreement with the model wind vectors
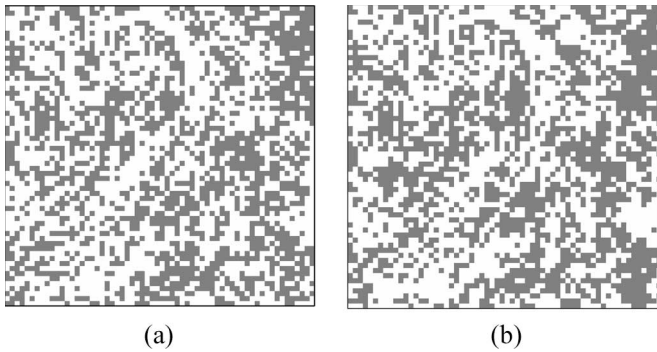
(a)   (b)

Fig. 5.   Channels giving rise to the best vector for each of the 3720 templates. Visible and infrared channels shown as gray and white, respectively. (a) MCC result of Fig. 4(e): 1620 visible and 2100 infrared. (b) Relaxed result of Fig. 4(f): 1718 visible and 2002 infrared.

TABLE I
ENTROPY OF MOTION FIELDS OF FIG. 4 (BITS/VECTOR)

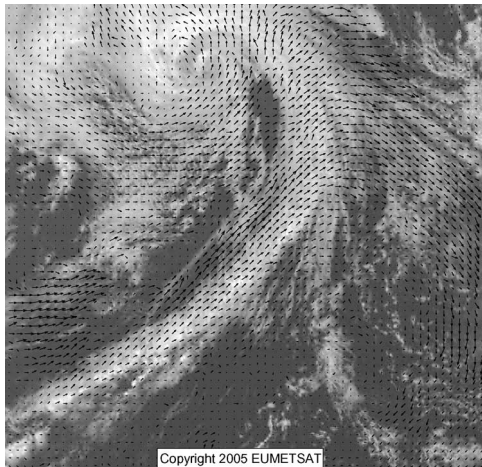| Image Channel	MCC Results	Relaxation Results
Visible	6.1339	3.5344
Infrared	6.4005	3.6882
Both Channels	5.9887	3.3554

Fig. 6.   Postfiltered result for Fig. 4(f): 80 of the 3720 vectors replaced with $\sigma = 250$ in (4) and a threshold $= 0.97$. Vectors at twice actual size for display purposes.

of Fig. 3. Here, 80 vectors were replaced, and the resulting motion field had an entropy of 3.1892 bits/vector.

Selecting candidate motion vectors that are good matches in both channels was also investigated by summing the CCCs from both channels before selecting the n best candidates. Compared with the results for both channels in Fig. 4(e) and (f), this approach produced a smoother MCC field, but its motion field after correlation-relaxation labeling was less smooth, resulting in 100 vectors being replaced by the post filter to produce a comparable result.

As a final assessment, the temporal consistency of the post-filtered motion fields was evaluated by comparing the result of Fig. 6 with the equivalent motion field produced using images from 12:15 UT and 12:30 UT on the same day. The root-mean-

square error between the two fields was 0.6476 pixels, with 82% of vectors having an error of < 1 pixel.

IV. CONCLUSION

A new multichannel approach to motion estimation has been presented. The technique was developed within the framework of correlation-relaxation labeling motion estimation, which has been shown to perform well for many remote sensing applications. Correlation-relaxation labeling is extended to accommodate vectors from more than one channel by allowing the vectors to compete at the initial selection of candidate vector sets. Other developments include an efficient support function, which only considers templates within a connected neighborhood, and a vector median postfilter.

The new technique was applied to MSG imagery, where the multichannel approach was shown to improve upon the results of any single channel for both the MCC and correlation-relaxation labeling techniques. Although the proposed approach does not assign heights to its vectors, it provides a dense, locally consistent motion field that appears to have much potential for techniques such as NWP. The extension of the technique to three dimensions and its incorporation into an NWP model is an area of ongoing research.

REFERENCES

[1] J. Schmetz, K. Holmlund, J. Hoffman, B. Strauss, B. Mason, V. Gaertner, A. Koch, and L. Van De Berg, "Operational cloud-motion winds from Meteosat infrared images," *J. Appl. Meteorol.*, vol. 132, no. 7, pp. 1206–1225, Jul. 1993.
[2] S. Côté and A. R. L. Tatnall, "A neural network-based method for tracking features from satellite sensor images," *Int. J. Remote Sens.*, vol. 16, no. 16, pp. 3695–3701, 1995.
[3] D. P. Mukherjee and S. T. Acton, "Cloud tracking by scale space classi- fication," *IEEE Trans. Geosci. Remote Sens.*, vol. 40, no. 2, pp. 405–415, Feb. 2002.
[4] Q. X. Wu, "A correlation-relaxation-labeling framework for computing optical flow: Template matching from a new perspective," *IEEE Trans. Pattern Anal. Mach. Intell.*, vol. 17, no. 9, pp. 843–853, Sep. 1995.
[5] Q. X. Wu, S. J. McNeill, and D. Pairman, "Correlation and relaxation labelling: An experimental investigation on fast algorithms," *Int. J. Remote Sens.*, vol. 18, no. 3, pp. 651–662, Feb. 1997.
[6] A. N. Evans, "On the use of ordinal measures for cloud tracking," *Int. J. Remote Sens.*, vol. 21, no. 9, pp. 1939–1944, Jun. 2000.
[7] L. Zhou, C. Kambhamettu, D. B. Goldgof, K. Palaniappan, and A. F. Hasler, "Tracking nonrigid motion and structure from 2D satellite cloud images without correspondences," *IEEE Trans. Pattern Anal. Mach. Intell.*, vol. 23, no. 11, pp. 1330–1336, Nov. 2001.
[8] C. S. Velden, T. L. Olander, and S. Wanzong, "The impact of multispectral goes-8 wind information on Atlantic tropical cyclone track forecasts in 1995. Part 1: Dataset methodology, description, and case analysis," *Mon. Weather Rev.*, vol. 126, no. 5, pp. 1202–1218, 1998.
[9] A. N. Evans, "Glacier surface motion computation from digital image sequences," *IEEE Trans. Geosci. Remote Sens.*, vol. 38, no. 2, pp. 1064–1072, Mar. 2000.
[10] J. Astola, P. Haavisto, and Y. Neuvo, "Vector median filters," *Proc. IEEE*, vol. 78, no. 4, pp. 678–689, Apr. 1990.
[11] ITU, *Recommendation H.263 (02/98)—Video Coding for Low Bit Rate Communication*, Int. Telecommun. Union, ITU-T H.263, 1998.